Sign reversal of the Hall response in a crystalline superconductor

Erez Berg,[1] Sebastian D. Huber,[2] and Netanel H. Lindner[3]
[1]*Department of Condensed Matter Physics, Weizmann Institute of Science, Rehovot 76100, Israel*
[2]*Theoretische Physik, Wolfgang-Pauli-Strasse 27, ETH Zurich, CH-8093 Zurich, Switzerland*
[3]*Department of Physics, Technion - Israel Institute of Technology, Haifa 32000, Israel*
(Received 11 March 2014; revised manuscript received 24 December 2014; published 15 January 2015)

We consider the Hall conductivity due to the motion of a vortex in a lattice model of a clean superconductor, using a combination of general arguments, unrestricted Hartree-Fock calculations, and exact diagonalization. In the weak-coupling limit, $k_F\xi \gg 1$, the sign of the Hall response of the superconducting state is the same as that of the normal (nonsuperconducting) state. For intermediate and strong coupling ($k_F\xi \sim 1$), however, we find that the sign of the Hall response in the superconducting state can be opposite to that of the normal state. In addition, we find that the sign reversal of the Hall response is correlated with a discontinuous change in the density profile at the vortex core. Implications for experiments in the cuprate superconductors are discussed.

DOI: 10.1103/PhysRevB.91.024507 PACS number(s): 74.25.N−, 74.25.fc, 74.25.Op, 74.78.−w

I. INTRODUCTION

The sign of the Hall response in a metal or semiconductor reveals the charge of the underlying charge carriers (electrons or holes). In the absence of a crystalline lattice or disorder, the Hall conductivity is fixed by Galilean invariance, and given by

$$\sigma_{xy} = \frac{nec}{B}, \tag{1}$$

where n is the electron density, c is the speed of light, B is the applied magnetic field, and e is the the electron charge. When a lattice is introduced, the Hall conductivity can deviate from (1), both in magnitude and in sign. The explanation of the Hall conductivity was one of the early successes of the Bloch theory of metals.

When a metal undergoes a superconducting transition, its Hall conductivity can change dramatically. Deep in the superconducting phase, if the superconducting vortices become pinned by disorder, the Hall resistance vanishes (as does the diagonal resistance). If the pinning is sufficiently weak (in clean samples, at high temperatures, or high magnetic fields), vortex motion leads to a finite Hall resistance. If we neglect the crystalline lattice, σ_{xy} is again fixed by Galilean invariance and given by (1); in the presence of a lattice or impurities, however, the magnitude and sign of the Hall response can differ from that of the normal (nonsuperconducting) state. A change in the sign of the Hall response upon approaching the superconducting phase has been detected in the cuprate superconductors in the underdoped [1–3] and optimally doped [4] regime. A similar phenomenon has been observed in conventional superconductor films [4].

The Hall response of a superconductor in the presence of disorder has been investigated thoroughly in the literature [5,6]. The effects of the crystalline lattice, however, have not been fully clarified. Traditionally, the problem has been analyzed phenomenologically in a time-dependent Ginzburg-Landau framework [7]. The key is to analyze the motion of a single superconducting vortex in the presence of a lattice and a background superflow [5,8,9]; this is a collective phenomenon in terms of the electrons (or Cooper pairs), and is thus not easy to describe.

In this paper, we study the Hall response of a microscopic model of a lattice superconductor. We follow the strategy of Refs. [10–12], which studied the Hall conductivity of interacting lattice bosons: the Hall conductivity of a system containing a single vortex is formulated as a property of the many-body wave function, which is calculated nonperturbatively in the interparticle interactions. We find a rich behavior of the Hall conductivity as a function of the number of electrons per unit cell, n, and the strength of the attractive interaction that leads to superconductivity, U (parametrized by the dimensionless number $k_F\xi$, where k_F is the Fermi momentum and ξ is the coherence length).

A representative phase diagram for the Hall conductivity is seen in Fig. 1. In the Bardeen-Cooper-Schrieffer (BCS) limit, $k_F\xi \gg 1$, we find that the Hall conductivity changes sign as a function of density at the point where the normal-state Fermi surface changes its topology from particle-like to hole-like. In this regime, therefore, the sign of the Hall response is the same as in the underlying normal state. When $k_F\xi$ is of the order of unity, however, the density at which σ_{xy} changes sign can be different from that of the normal state. A nonmonotonic behavior of this critical density as a function of $k_F\xi$ is found. In a certain range of densities, the Hall conductivity changes its sign as a function of temperature upon cooling from the normal to the superconducting state. We discuss the origin of this behavior, and possible implication for short coherence length superconductors, such as the cuprates.

II. MODEL

We consider a model of interacting electrons hopping on a square lattice. The Hamiltonian is given by

$$H = -\sum_{\vec{r},\vec{r}',\sigma=\uparrow,\downarrow} t^{\sigma}_{\vec{r}\vec{r}'} c^{\dagger}_{\vec{r}\sigma} c_{\vec{r}'\sigma} + \text{H.c.} + \sum_{\vec{r}} \left[-U \left(n_{\vec{r}\uparrow} - \frac{1}{2} \right) \left(n_{\vec{r}\downarrow} - \frac{1}{2} \right) - \mu n_{\vec{r}} \right]. \tag{2}$$

Here, $c_{\vec{r}\sigma}$ annihilates an electron on site $\vec{r}$ with spin σ, $n_{\vec{r}\sigma} = c^{\dagger}_{\vec{r}\sigma} c_{\vec{r}\sigma}$, and $n_{\vec{r}} = n_{\vec{r}\uparrow} + n_{\vec{r}\downarrow}$. The hopping parameters are chosen to be $t^{\sigma}_{\vec{r}\vec{r}'} = t e^{ieA^{\sigma}_{\vec{r}\vec{r}'}}$ for nearest-neighbor sites, $t^{\sigma}_{\vec{r}\vec{r}'} = t' e^{ieA^{\sigma}_{\vec{r}\vec{r}'}}$ for next-nearest neighbors, and 0 otherwise. (We choose in units such that $\hbar = c = 1$.) The spin-dependent

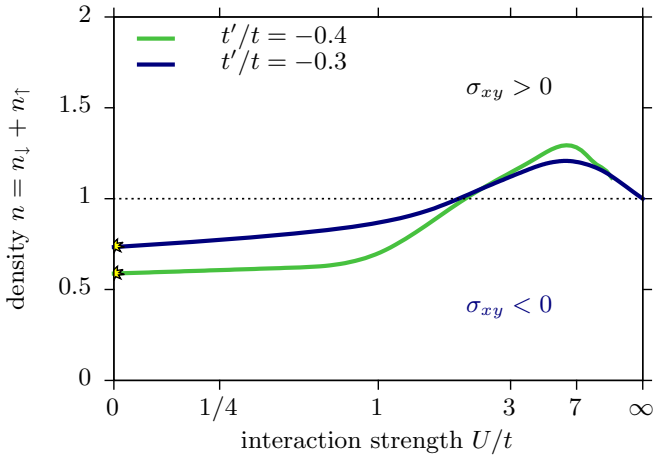

FIG. 1. (Color online) Phase diagram. The Hall conductivity is given by $\sigma_{xy} = \frac{e^2}{2\pi}(n - 2p)$ with $p \in \mathbb{Z}$ and ρ denoting the density. The line indicates the location where p changes from zero to one and therefore signals a sign change in σ_{xy}. The stars at $U = 0$ mark the location of the Van Hove singularities.

gauge field $A^{\sigma}_{\vec{r}\vec{r}'}$ is introduced in order to induce vortices in the system, and will be defined below. U is an on-site attractive interaction. When $U > 0$ (which we assume in the following) and $\mu \neq 0$, the ground state of H in Eq. (2) is superconducting for all values of U, crossing over smoothly from the BCS limit $U \ll \max\{|t|,|t'|\}$ to a Bose-Einstein condensate of tightly bound pairs in the large-U limit. To suppress a competing charge-ordering instability, it will sometime be useful to add an extended interaction term $H_V = V \sum_{\langle ij \rangle}(n_i - 1)(n_j - 1)$, where $\langle i, j \rangle$ are nearest-neighbor sites.

III. COMPUTATION OF σ_{xy}

In order to calculate σ_{xy} due to the motion of a single vortex, we define the lattice model on a torus of size $L_x \times L_y$. Next, we need to choose the gauge field A^{σ}_{ij}. The flux of the gauge field $A^{\sigma}_{\vec{r}\vec{r}'}$ through the system is quantized to $2\pi N^{\sigma}_{\phi}$, where N^{σ}_{ϕ} are integers. The ground state is a condensate of Cooper pairs, composed of one electron of each spin species; therefore, the total flux seen by the condensate is $2\pi(N^{\uparrow}_{\phi} + N^{\downarrow}_{\phi})$. We see that if $N^{\uparrow}_{\phi} = N^{\downarrow}_{\phi}$, the total number of superconducting flux quanta is an even integer. Then, there are at least two vortices on the torus, and the analysis of the contribution of a single vortex to σ_{xy} is complicated by intervortex interactions.

Alternatively, we may choose $\{N^{\uparrow}_{\phi}, N^{\downarrow}_{\phi}\} = \{1,0\}$, for which there is a single vortex on the torus. This choice may look odd at first glance, since it does not correspond to a physical magnetic field. Nevertheless, we argue that it captures correctly the contribution of a single vortex to σ_{xy} in the limit $L_x, L_y \gg \xi$. To understand why, we note that the magnetic field in the vortex core region is small. As we will argue in the following, the Hall conductivity is determined by the structure of the core. Therefore, in the limit of large system size, the only role of the external magnetic field is to guarantee that the ground state has a single vortex; the dynamics of the vortex is independent of the precise way it was induced.

In the following, we set $A^{\downarrow}_{\vec{r}\vec{r}'} = 0$, and choose $A^{\uparrow}_{\vec{r}\vec{r}'}$ such that electrons with spin up are subject to a uniform flux of $2\pi/L_x L_y$ per unit cell. An explicit gauge choice for $A^{\uparrow}_{\vec{r}\vec{r}'}$ is shown in Appendix A. We imposed twisted boundary conditions such that the electron operators satisfy and $c_{\vec{r}+L_\alpha \hat{e}_\alpha,\sigma} = e^{i\Theta_\alpha} c_{\vec{r},\sigma}$ for $\alpha = x, y$.

The Hall conductivity of the system at $T = 0$ may then be expressed as [13,14]

$$\sigma_{xy} = \frac{e^2}{(2\pi)^2} \int_0^{2\pi} \int_0^{2\pi} d\Theta_x d\Theta_y \mathrm{Im}\langle \partial_{\Theta_x} \Psi | \partial_{\Theta_y} \Psi \rangle, \qquad (3)$$

where $|\Psi(\Theta_x, \Theta_y)\rangle$ is the many-body ground state wave function, which depends on the boundary conditions. Equation (3) requires that $|\Psi(\Theta_x, \Theta_y)\rangle$ be unique for all $(\Theta_x, \Theta_y) \in [0, 2\pi]$, as is generically the case for our finite-size system. Then, σ_{xy} is quantized in units of $e^2/2\pi$.

Equation (3) relates σ_{xy} to the Berry phase accumulated when Θ_x, Θ_y are changed adiabatically. Changing Θ_x, Θ_y moves the position of the center of mass of the vortex on the torus [12], so the Hall conductivity per site can be viewed as the Berry phase Φ_B associated with the adiabatic motion of the vortex core around a *single unit cell*. This Berry phase is related by a "generalized Luttinger theorem" to the density of charged particles in the system [12,15,16]:

$$\Phi_B = 2\pi \left(\frac{n}{2} + p \right), \qquad (4)$$

where $n = n_\uparrow + n_\downarrow$ is the mean number of charge e particles per unit cell, and p is an integer. (For more details, see Appendix B.) As $\Theta_{x,y}$ is changed by π, the vortex core moves by $L_{x,y}$ in the x or y direction, respectively [11,12] (note that $\Theta_{x,y}$ twists the boundary condition for both spin flavors). Therefore, Eq. (3) can be expressed as $\sigma_{xy} = \frac{e^2}{(2\pi)^2} 4 L_x L_y \Phi_B$.

In the absence of a crystalline lattice, $p = 0$; Eq. (4) then reproduces the well-known result for the Berry phase associated with the motion of a vortex in a superfluid in free space [17]. In that case, the Berry phase is directly related to the effective Lorentz force exerted on a moving vortex: $\vec{F}_L = \nu \Phi_B \hat{z} \times \vec{u}_v$, where $\nu = \pm 1$ is the vorticity of the vortex and $\vec{u}_v$ is its velocity. In a lattice system, however, the force on a vortex is, strictly speaking, an ill-defined concept. Nevertheless, the connection of Eq. (4) to the Hall conductivity of a single vortex, through Eq. (3), is still valid.

Upon varying parameters of the Hamiltonian (2), the integer p can only change discontinuously via a level crossing in the many-body spectrum, at which the integrand of Eq. (3) is ill defined. Since far away from the vortex core the system is gapped [18], any level crossing must occur within the vortex core. In the following, we will focus our attention to the vortex core and map out the location of the jumps of the integer p in Eq. (4).

IV. GENERAL ARGUMENTS

We are interested in σ_{xy} as a function of the electron density n [tuned by the chemical potential in Eq. (2)], the interaction strength U/t, and the next-nearest neighbor hopping t'/t. Below, we discuss general arguments that can be used to constrain the form of σ_{xy} as a function of model parameters.

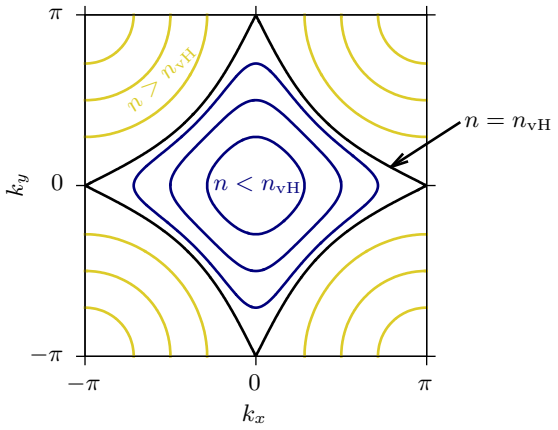

FIG. 2. (Color online) Fermi surface for $U = 0$ and $t'/t = -0.3$ at different densities n, relative to the density of the Van Hove singularity, $n_{\rm VH}$.

Let us first discuss the case $t' = 0$. Then, under a particle-hole transformation $\mathcal{C}$ defined through $\mathcal{C}_Q c_{\vec{r},\sigma} \mathcal{C}_Q^{-1} = e^{i\vec{Q}\cdot\vec{r}} c^\dagger_{\vec{r},\sigma}$ where $\vec{Q} = (\pi,\pi)$, the Hamiltonian satisfies $H(\mu) = H^*(-\mu)$. Because of the complex conjugation operation, σ_{xy} is odd under $\mathcal{C}_Q$: $\sigma_{xy}(\mu,U/t) = -\sigma_{xy}(-\mu,U/t)$. Under $\mathcal{C}_Q$, $n \to 2 - n$; therefore, σ_{xy} must change its sign at $n = 1$ for any value of U/t. This change of sign occurs through a jump in the integer p in Eq. (4), which is associated with a degeneracy at the vortex core.

For $t' \neq 0$, particle-hole symmetry is broken, and the critical density n_c at which p jumps (and σ_{xy} changes sign) can depend on U/t. Nevertheless, in the extreme limits of weak and strong coupling, the position of the jump can be deduced from the following arguments. For $U/t = 0$, the system is noninteracting with a single-particle dispersion given by $\varepsilon_{\vec{k}} = -2t(\cos k_x + \cos k_y) - 4t' \cos k_x \cos k_y - \mu$. The ground state is a filled Fermi sea. The Fermi surface undergoes a Van Hove singularity at $\mu = 4t'$ (corresponding to a density $n_{\rm VH}$), changing its character from a particle-like to a hole-like Fermi surface (see Fig. 2). By standard semiclassical reasoning [19], σ_{xy} is expected to change sign at $n = n_{\rm VH}$. Continuity implies that in the limit $U/t \to 0, n_c(U/t) \to n_{\rm VH}$. In Appendix C, we show that n_c indeed changes continuously in the limit $U/t \to 0$ and approaches $n_{\rm VH}$, by analyzing the spectrum of a vortex core in the weak-coupling limit.

In the opposite limit, $U/t \gg 1$ (keeping t'/t fixed), n_c can also be easily determined. To zeroth order in t/U, there are infinitely many degenerate ground states, corresponding to an occupation of either zero or two electrons in every site. Expanding in powers of t/U, one obtains the following effective hard-core boson Hamiltonian:

$$H_b = -\sum_{\vec{r},\vec{r}'} \tilde{t}_{\vec{r},\vec{r}'} b^\dagger_{\vec{r}} b_{\vec{r}'} + \text{H.c.} - 2\mu \sum_{\vec{r}} n_{b,\vec{r}} + \sum_{\vec{r},\vec{r}'} \tilde{V}_{\vec{r},\vec{r}'} \left(n_{b,\vec{r}} - \frac{1}{2}\right)\left(n_{b,\vec{r}'} - \frac{1}{2}\right) + O\left(\frac{t^3}{U^2}\right), \tag{5}$$

where $b^\dagger_{\vec{r}}$ creates a pair of electrons with opposite spins on site $\vec{r}$, $n_{b,\vec{r}} = b^\dagger_{\vec{r}} b_{\vec{r}}$, and $\tilde{t}_{\vec{r},\vec{r}'}$, $\tilde{V}_{\vec{r},\vec{r}'}$ are effective boson hopping and interaction, which scale as t^2/U. Explicit expressions for $\tilde{t}_{\vec{r},\vec{r}'}$, $\tilde{V}_{\vec{r},\vec{r}'}$, as well as higher order terms in t/U, are given in Appendix E.

To order t^2/U, the system is particle-hole symmetric: $\mathcal{C}_B H_b(\mu) \mathcal{C}_B^{-1} = H_b(-\mu)$, *independently of* t'/t, where $C_B b_{\vec{r}} C_B^{-1} = b^\dagger_{\vec{r}}$. This fixes $n_c(U/t \to \infty) = 1$, up to corrections of higher order in t/U: Particle-hole symmetry breaking terms appear in Eq. (5) at order t^3/U^2, and their sign depends on the sign of t'. In Appendix E, we analyze the correction to $n_c(U/t)$ due to these terms, and find that for positive (negative) t', $n_c(U/t)$ approaches 1 from below (above) in the $U/t \to \infty$ limit. This is supported by our numerical calculations which we discuss next.

V. NUMERICAL CALCULATIONS

In the intermediate interaction regime, $U/t \sim 1$, we lack a small expansion parameter and therefore resort to a numerical calculation of Φ_B. We apply an unrestricted Hartree-Fock approximation by minimizing the energy $\langle\Psi(\{\Delta_{\vec{r}},\mu_{\vec{r}\sigma}\})|H|\Psi(\{\Delta_{\vec{r}},\mu_{\vec{r}\sigma}\})\rangle$ where $|\Psi(\{\Delta_{\vec{r}},\mu_{\vec{r},\sigma}\})\rangle$ is the ground state of the trial Hamiltonian

$$H_{\rm HF} = -\sum_{\vec{r},\vec{r}',\sigma=\uparrow,\downarrow} t^\sigma_{\vec{r}\vec{r}'} c^\dagger_{\vec{r}\sigma} c_{\vec{r}'\sigma} + \text{H.c.} + \sum_{\vec{r}} \Delta^*_{\vec{r}} c_{\vec{r}\uparrow} c_{\vec{r}\downarrow} + \text{H.c.} - \sum_{\vec{r},\sigma=\uparrow,\downarrow} \mu_{\vec{r}\sigma} n_{\vec{r}\sigma}. \tag{6}$$

We determine the (self-consistent) variational parameters $\{\Delta_{\vec{r}},\mu_{\vec{r}\sigma}\}$ via iteration. For the numerical results presented below, we use lattices up to a size of $L_x \times L_y = 50 \times 50$, such that $L_{x,y} \gg \xi$.

In Fig. 3 we show the resulting gap $\Delta_{\vec{r}}$ and density $n_{\vec{r}}$ profiles. We confirm that for the gauge field $A^\uparrow_{\vec{r}\vec{r}'}$ a topological defect in the phase field of $\Delta_{\vec{r}}$ is stabilized. The location of the vortex is determined by the boundary conditions. For the figure we use $(\Theta_x,\Theta_y) = 2\pi/L \times (10,10)$, which in our gauge (Appendix A) leads to a location of the vortex $\vec{r}_{\rm V} = (10,10)$.

By varying the boundary conditions (Θ_x,Θ_y) we can calculate the Chern number of the many-body ground state $|\Psi(\{\Delta_{\vec{r}},\mu_{\vec{r}\sigma}\})\rangle$ using Eq. (3). (The calculation of overlaps of BdG wave functions is discussed in Appendix D.) Our results are in accordance with the rule (4), relating Φ_B to the density up to an integer. As the density is increased at a fixed value of U/t, the integer p changes abruptly from 0 to -1 at a critical density $n_c(U/t)$. Figure 1 shows n_c as a function of U/t, for different values of the second-neighbor hopping amplitude t'. The integer p takes the value 0 (-1) for densities below (above) n_c, corresponding to negative (positive) σ_{xy}, respectively. As expected, for $U/t \ll 1$, $n_c \to n_{\rm VH}$, while for $U/t \gg 1$, $n_c \to 1$. The critical density has a different asymptotic behavior for $U \ll t$ and $U \gg t$: $n_c(U/t \to 0) < 1$ while $n_c(U/t \to \infty) > 1$. Hence, we find that $n_c(U/t)$ has a nonmonotonic dependence on U/t.

Figure 3 shows the density and pairing potential profiles for two solutions on either side of the critical density $n_c(U/t)$. While the pairing potential profiles look similar, the density

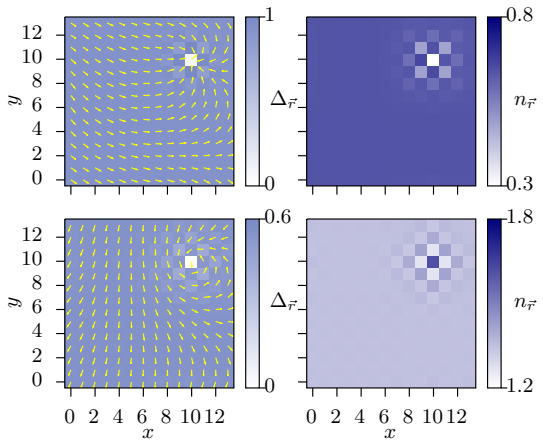

FIG. 3. (Color online) Vortex cores. Order parameter (left panels) and density profiles (right panels) for $U/t = 3$, $V/t = -0.05$, $t'/t = -0.3$, $L_x = L_y = L = 14$. In the left panels the color indicates the amplitude of the order parameter while the arrow indicates its phase. In the right panels the color reflects the total density. (a) Particle-like superconductor at $n \approx 0.63$ where the vortex core nucleates a charge density wave with a depleted site at the vortex core. Here $\sigma_{xy} < 0$. (b) Hole-like superconductor at $n \approx 1.35$ with a charge density wave where the central site carries an excess density and $\sigma_{xy} > 0$. In both cases the vortex was centered on a site by using fluxes through the openings of the torus $(\Theta_x, \Theta_y) = (10, 10) \times 2\pi/L$.

profiles show a clear distinction: Below the critical density [$n < n_c$, panel (a)], the vortex core is *depleted*, while the situation is reversed above the critical density [$n > n_c$, panel (b)], where the core carries an *excess density*. These two solutions cross in energy at $n_c(U/t)$. Such a level crossing indicates a possible change in the Chern number (3) and hence the Berry phase Φ_B. Note that the density in the core is modulated with a wave vector $Q \sim (\pi, \pi)$. This is a result of the competing charge density wave (CDW) instability for a Fermi surface which exhibits some amount of nesting near half filling; cf. Fig. 2. In a homogeneous system, the CDW instability is suppressed by the superconducting order. At the vortex core, however, the vanishing of the gap $\Delta_{\vec{r}_V}$ promotes the CDW locally [20].

VI. FINITE TEMPERATURE

The zero-temperature results, summarized in Fig. 3, show that there is a range of densities near half filling at which the sign of σ_{xy} in the superconductor is different from the normal state. Within this range, one expects also a sign change in σ_{xy} when we destroy superconductivity by raising temperature at a fixed value of U/t. We now generalize our approach to address the temperature dependence of σ_{xy}.

We use a thermal state of Hamiltonian (6) to determine self-consistently the parameters $\{\Delta_{\vec{r}}, \mu_{\vec{r}\sigma}\}$. Then, one can calculate the thermally averaged Chern number [11]

$$\sigma_{xy}(T) = \sum_{\alpha} \frac{e^2}{(2\pi)^2} \int_0^{2\pi} d\Theta_x d\Theta_y e^{-\frac{E_\alpha}{k_B T}} \mathrm{Im}\langle \partial_{\Theta_x} \Psi_\alpha | \partial_{\Theta_y} \Psi_\alpha \rangle,$$

where α runs over all excited states. Figure 4 summarizes our results for one density $n \approx 1$ at $t'/t = -0.3$ and $V/t = -0.05$.

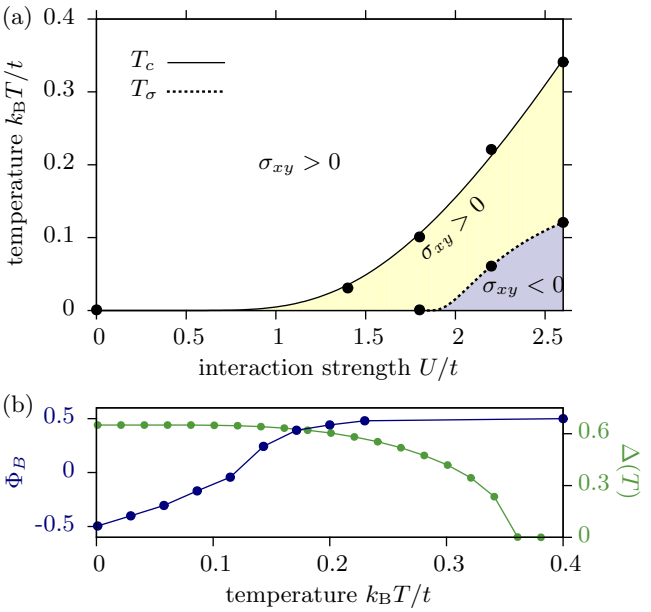

FIG. 4. (Color online) Finite temperature. In panel (b) we show the dependence of the order parameter Δ as well as the Berry phase Φ_B as a function of temperature for $U/t = 2.6$, $t'/t = -0.3$, $V/t = -0.05$, and $n \approx 1$. The change in sign in Φ_B below T_c is apparent and its location defines T_σ. In panel (a) we show a phase diagram for $n \approx 1$ with T_c and T_σ indicated showing that there is a sign change in σ_{xy} *within* the superconducting region. Lines in panel (a) are a guide to the eye.

In panel (b) we show one temperature trace of Φ_B evaluated in a thermal ensemble for $U/t = 2.6$. We see that Φ_B changes its sign before the order parameter vanishes, i.e., within the superconductor. Moreover, we see that the sharp jump at $T = 0$ is washed out by thermally excited states. We can now define the temperature T_σ where Φ_B changes sign and T_c where superconductivity is lost. Panel (a) shows a phase diagram that summarizes our finite-temperature results.

VII. DISCUSSION

We have analyzed the Hall response of a lattice-superconductor, by examining the motion of a single vortex in a background superflow. By combining general arguments with numerical simulations, we have shown that in the vicinity of half filling, it is possible to find situations where the normal-state Hall response is *opposite in sign* compared to that of the superconducting ground state, leading to a sign change in σ_{xy} as a function of temperature. Unlike previously proposed mechanisms, the present mechanism is an effect of the crystalline lattice, and does not disappear in the clean limit.

It would be interesting to generalize our results to models applicable to the cuprate superconductors. In particular, one needs to include the d-wave symmetry of the order parameter and the strong correlations due to on-site repulsive interactions. Interestingly, the density of carriers in the hole-doped cuprates satisfies $n_{\mathrm{VH}} < n < 1$. Therefore, within the simple model used here, it lies in the range in which the sign of σ_{xy} in the superconductor at intermediate coupling is different from that of the normal state.

ACKNOWLEDGMENTS

We thank A. Auerbach, G. Blatter, B. Halperin, V. Kalnizky, and S. Sachdev for useful discussions. S.H. acknowledges support from the Swiss National Science Foundation. E.B. was supported by the Israel Science Foundation, by the Israel-USA Binational Science Foundation, by the Minerva Foundation, by a Marie Curie CIG grant, and by the Robert Rees Fund. N.L. acknowledges support from I-CORE, the Israeli Center of Research Excellence: "Circle of Light". This work was supported in part by National Science Foundation Grant No. PHYS-1066293 and the hospitality of the Aspen Center for Physics as well as the Pauli Center for Theoretical Studies.

APPENDIX A: CHOICE OF GAUGE

In Fig. 5 we show the Landau gauge we used for the numerical calculations. The arrow indicate the phases picked up by the $\uparrow$ electrons when hopping over the respective link. The arrows denote the following values:

$$\rangle = \frac{\Phi}{2L_x L_y} \quad \text{and} \quad \rangle = 2L_x \times \rangle, \tag{A1}$$

where L_x is the extent of the lattice in the horizontal direction in Fig. 5 and $\Phi = 2\pi$ for one vortex.

Note that at the right edge of the lattice there is a winding of 2π for the hopping in the horizontal direction (blue arrows). When comparing to the phase pattern $\phi(\vec{r}) = \arg[\Delta(\vec{r})]$ of the superconducting order parameter in Fig. 3 of the paper, we see that the gauge-invariant current $j \sim \nabla\phi(\vec{r}) - e\vec{A}(\vec{r})$ is indeed continuous [11].

APPENDIX B: VORTEX BERRY PHASE AND THE HALL CONDUCTIVITY

In the following we clarify the origin of the "generalized Luttinger theorem" for the Berry phase accumulated when taking a vortex around a single unit cell. First, consider twisting only the boundary condition for the spin-up electrons by $\Theta^{\uparrow}_{x,y}$, by defining the gauge field as

$$A^{\uparrow}_{\vec{r}\vec{r}'} = (A_L)^{\sigma}_{\vec{r}\vec{r}'} + \left(\frac{\Theta^{\uparrow}_x}{L_x}, \frac{\Theta^{\uparrow}_y}{L_y}\right) \cdot (\vec{r} - \vec{r}')/|\vec{r} - \vec{r}'|, \tag{B1}$$

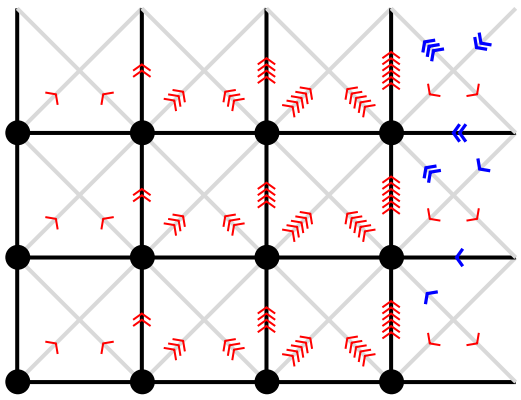

FIG. 5. (Color online) Gauge choice.

where $(A_L)^{\sigma}_{\vec{r}\vec{r}'}$ is the gauge field configuration appearing in Fig. 5. In this case, changing $\Theta^{\uparrow}_{x,y}$ by $2\pi/L_{x,y}$ moves the vortex by one lattice site in the x or y direction [11,12]. Moreover, such a change in $\Theta^{\uparrow}_{x,y}$ gives a Hamiltonian which is unitarily equivalent to the original one. Therefore, a similar construction to the one appearing in Ref. [12] yields a "generalized Luttinger theorem" which gives the Berry phase acquired when taking the vortex around a single unit cell as

$$\Phi_B = 2\pi(n_{\uparrow} + p). \tag{B2}$$

In the model analyzed in this paper, $n_{\uparrow} = n_{\downarrow} = n/2$.

Now consider twisting the boundary conditions for both spin values $\Theta^{\uparrow}_{x,y} = \Theta^{\downarrow}_{x,y} = \Theta_{x,y}$. The vortex moves by one lattice site upon changing $\Theta_{x,y}$ by $\pi/L_{x,y}$ (as a Cooper pair is twisted by $2\Theta_{x,y}$). When $L_x, L_y \gg \xi$, we expect the Berry phase accumulated when moving the vortex around a single unit cell using a twist for both spin flavors to also give Φ_B as in Eq. (B2). This is indeed verified by our numerical calculations. Therefore, for $L_x, L_y \gg \xi$, we obtain the relation between the Hall conductivity and Φ_B as

$$\sigma_{xy} = \frac{4e^2}{(2\pi)^2} L_x L_y \Phi_B. \tag{B3}$$

APPENDIX C: WEAK-COUPLING LIMIT

For noninteracting electrons, semiclassical reasoning [19] shows that the sign of σ_{xy} is determined by the topology of the Fermi surface. For an electron-like (a hole-like) Fermi surface, σ_{xy} is negative (positive), respectively. In the limit $U/t \ll 1$, one may expect σ_{xy} to approach its noninteracting value, and hence $n_c(U/t) \to n_{\mathrm{VH}}$ as $U/t \to 0$. This is not entirely obvious, however, since the ground state changes its nature singularly in the limit $U \to 0$. In this section, we show explicitly that σ_{xy} is indeed smooth for $U \to 0$.

By the arguments in the main text, the critical density n_c in which σ_{xy} changes sign is associated with a level crossing at the vortex core. Let us analyze the spectrum of Marticon–Caroli–de Gennes (MCdG) states in the core. The Bogoliubov–de Gennes (BdG) Hamiltonian is of the form

$$H_{\mathrm{BdG}} = \varepsilon(\vec{k})\tau^z + \Delta(\vec{r})\,\tau^+ + \mathrm{H.c.}, \tag{C1}$$

where $\varepsilon(\vec{k})$ is a general energy dispersion as a function of the crystal momentum $\vec{k}$, $\Delta(\vec{r} = i\vec{\nabla}_k)$ is a pairing potential that includes a vortex at $\vec{r} = \vec{r}_V$, and $\vec{\tau}$ are Pauli matrices acting in Nambu space on the spinor $\psi^T_{\vec{k}} = (c_{\vec{k},\uparrow}, c^{\dagger}_{-\vec{k},\downarrow})$. We assume that the system is defined on a square lattice, such that $\varepsilon(\vec{k})$ is symmetric under C_4. The Fermi surface is at $\varepsilon(\vec{k}) = 0$. For simplicity, let us consider a linear gap function which describes a vortex at $\vec{r}_V = 0$:

$$\Delta(\vec{r}) = \frac{\Delta_0}{\xi}(x - iy), \tag{C2}$$

where Δ_0 and ξ are parameters. The precise gap profile is not expected to change our results qualitatively.

We now transform the coordinates to a new frame $(k_{\parallel}, k_{\perp})$ such that $k_{\parallel}$ ($k_{\perp}$) is parallel (perpendicular) to the Fermi surface, respectively. The transformation is depicted in Fig. 6(a).

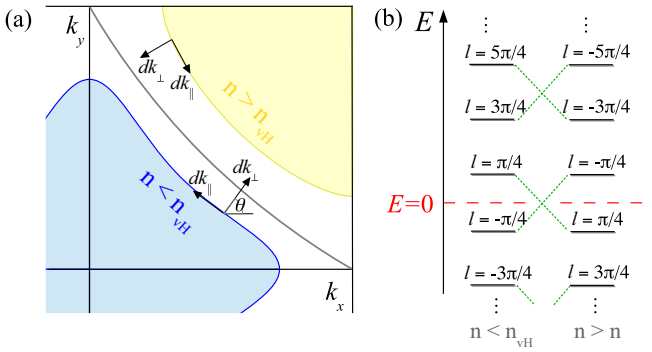

FIG. 6. (Color online) (a) Transformation to the Fermi surface coordinates $(k_\parallel,k_\perp)$ defined via Eq. (C3). (b) Spectrum of the BdG Hamiltonian (C6), on either side of the Van Hove density $n_{\rm VH}$. The states are labeled by l, their angular momentum under rotation by $\pi/2$ (defined mod2π). The fine dashed lines show the schematic evolution of the spectrum as n is varied across $n_{\rm VH}$.

The new coordinates are related to the old ones by

$$dk_x = \cos\theta dk_\perp - J\sin\theta dk_\parallel,$$
$$dk_y = \sin\theta dk_\perp + J\cos\theta dk_\parallel. \tag{C3}$$

Here, $\theta(k_\parallel/k_p)$ is the angle between the normal to the Fermi surface and the horizontal axis (k_p is the perimeter of the Fermi surface), and J is the Jacobian of the transformation. We fix the orientation of $k_\parallel$ by requiring

$$\int_0^{k_p} dk_\parallel \frac{d\theta}{dk_\parallel} = +2\pi. \tag{C4}$$

Since Eqs. (C3) must be total differentials, we find that $\partial_{k_\perp} J = \partial_{k_\parallel}\theta$. The following choice of J is consistent with this constraint:

$$J(k_\perp,k_\parallel) = 1 + \frac{k_\perp}{k_p}\theta'\left(\frac{k_\parallel}{k_p}\right). \tag{C5}$$

Performing the coordinate transformation (C3), linearizing the dispersion near the Fermi surface, and finally performing a similarity transformation $H_{\rm BdG} \to \tilde{H}_{\rm BdG} = J^{1/2}UH_{\rm BdG}U^{-1}J^{-1/2}$ where $U = \exp[i\theta\tau^z/2]$, the BdG Hamiltonian takes the form

$$\tilde{H}_{\rm BdG} = H_\parallel + H_\perp, \tag{C6}$$

where

$$H_\parallel = \frac{\Delta_0}{\xi}\left(\frac{-i}{J}\right)\tau^y\left(\partial_{k_\parallel} + \frac{1}{2J}\frac{\partial J}{\partial k_\parallel}\right),$$
$$H_\perp = \frac{\Delta_0}{\xi}\tau^x i\partial_{k_\perp} + v_F(k_\parallel)k_\perp\tau^z. \tag{C7}$$

Here, $v_F(k_\parallel) = \nabla_k\varepsilon(k_\perp = 0)\cdot\hat{n}_\perp$ is the Fermi velocity, where $\hat{n}_\perp = (\cos\theta,\sin\theta)$ is the unit vector normal to the Fermi surface. Note that due to the unitary transformation U, the eigenstates of (C6) satisfy *antiperiodic* boundary conditions as a function of $k_\parallel$.

Anticipating $H_\parallel/\Delta_0 \sim \xi^{-1}\partial_{k_\parallel} \sim (k_p\xi)^{-1} \ll 1$, we diagonalize $\tilde{H}_{\rm BdG}$ perturbatively in $H_\parallel$. To zeroth order in $H_\parallel$, $\tilde{H}_{\rm BdG}$ has a family of zero modes parametrized by $k_\parallel$, of the form

$$\varphi(k_\perp,k_\parallel) = \varphi_0[k_\perp a(k_\parallel)]\begin{pmatrix}1\\ -i\,\mathrm{sgn}(v_F)\end{pmatrix}. \tag{C8}$$

Here, $\varphi_0(x) = \sqrt{2/\pi}e^{-x^2/2}$ is the harmonic oscillator ground state wave function, and we have defined $a(k_\parallel) = \sqrt{v_F(k_\parallel)\xi/2\Delta_0}$. Note that away from the Van Hove point, $v_F \neq 0$ for all $k_\parallel$, and therefore $\mathrm{sgn}(v_F)$ is independent of $k_\parallel$.

$H_\parallel$ lifts the degeneracy within the zero-energy subspace of $H_\perp$. Inserting $\psi(k_\parallel,k_\perp) = \chi(k_\parallel)\varphi(k_\perp,k_\parallel)$ into the eigenvalue equation for $\tilde{H}_{\rm BdG}$ and projecting both sides onto the subspace of zero modes defined by Eq. (C8), we get the following eigenvalue equation for χ [to leading order in $(\xi k_p)^{-1}$]:

$$\frac{\Delta_0}{\xi}i\,\mathrm{sgn}(v_F)\left(\partial_{k_\parallel} - \frac{1}{a}\frac{\partial a}{\partial k_\parallel}\right)\chi(k_\parallel) = E\chi(k_\parallel). \tag{C9}$$

The eigenstates are of the form $\chi_n = a(k_\parallel)\exp[ik_\parallel/q_n]$, where $1/q_n = \pi(2n+1)/k_p$, $n \in \mathbb{Z}$, and the corresponding eigenenergies are $E_n = -\frac{\Delta_0}{\xi q_n}\mathrm{sgn}(v_F)$. These are nothing but the well-known MCdG states, whose minimum energy is $\frac{\Delta_0}{\xi k_p} \sim \Delta_0^2/E_F$ (where we have used the estimates $\xi \sim v_F/\Delta_0$ and $E_F \sim v_F k_p$).

Now, let us consider the low-energy spectrum on either side of the Van Hove point, in which the Fermi surface undergoes a change of topology. According to our definition of the orientation of the Fermi surface, Eq. (C4), $\mathrm{sgn}(v_F) > 0$ for a particle-like Fermi surface ($n < n_{\rm VH}$), while $\mathrm{sgn}(v_F) < 0$ for a hole-like Fermi surface ($n > n_{\rm VH}$). Therefore, we see that across the Van Hove point, the two states χ_{-1} and χ_0 interchange their energy. These two states transform differently under C_4 (e.g., under rotation by $\pi/2$, χ_0 and χ_{-1} pick up phases of $e^{\pm i\pi/4}$, respectively). Hence, $\chi_{0,-1}$ cannot hybridize with each other. We conclude that as the density crosses $n_{\rm VH}$, there must be a level crossing between χ_{-1} and χ_0.

More generally, under rotation by $\pi/2$, χ_n acquires a phase of $\exp[il_n]$, where $l_n = (2n+1)\pi/4$. Near the Van Hove point, χ_{2n-1} and χ_{2n} cross in energy. The distance from the level crossing point to the Van Hove point goes to zero in the weak-coupling limit, $k_p\xi \to \infty$. The spectrum on either side of the Van Hove point is shown in Fig. 6(b).

In terms of the many-body spectrum, a zero-energy state in the BdG spectrum corresponds to a level crossing between the ground state and the first excited state. Since the Chern number can only change via a level crossing, this implies that in the weak-coupling limit, the jump in the Hall conductivity occurs arbitrarily close to the Van Hove point. This conclusion is consistent with our numerical simulations (Fig. 1 in the main text).

Note that our argument relies on the presence of a C_4 symmetry. Indeed, if the C_4 symmetry is broken, there is generically no single Van Hove density in which the Fermi surface changes its character from particle-like to hole-like. The regions of electron and hole-like Fermi surfaces are generically separated by a density range with an open Fermi surface, in which the normal-state Hall conductivity is ill defined in the clean limit.

APPENDIX D: OVERLAPS OF BOGOLIUBOV–DE GENNES WAVE FUNCTIONS

In order to calculate Chern numbers [Eq. (3) of the main text], we need to compute overlaps of many-body wave functions. In the Hartree-Fock approximation, these wave functions are ground states of a variational quadratic Hamiltonian [Eq. (6) in the main text]. In order to derive a formula for the overlap between two such wave functions, it is convenient to perform a particle-hole transformation on one of the spin species:

$$\begin{aligned} c_{\vec{r}\uparrow} &= d_{1,\vec{r}}, \\ c_{\vec{r}\downarrow} &= d^{\dagger}_{2,\vec{r}}. \end{aligned} \tag{D1}$$

In terms of the new operators $d_{1,2}$, H_{HF} has the form

$$\begin{aligned} H_{\mathrm{HF}} = &- \sum_{\vec{r},\vec{r}',\sigma=\uparrow,\downarrow} (t^{\sigma}_{\vec{r}\vec{r}'} d^{\dagger}_{1,\vec{r}} d_{1,\vec{r}'} - t^{\downarrow}_{\vec{r}\vec{r}'} d^{\dagger}_{2,\vec{r}} d_{2,\vec{r}'} + \mathrm{H.c.}) \\ &- \sum_{\vec{r}} \Delta^{*}_{\vec{r}}\, d^{\dagger}_{2,\vec{r}} d_{1,\vec{r}} + \mathrm{H.c.} \\ &- \sum_{\vec{r},\sigma=\uparrow,\downarrow} (\mu_{\vec{r}\uparrow} d^{\dagger}_{1,\vec{r}} d_{1,\vec{r}} - \mu_{\vec{r}\downarrow} d^{\dagger}_{2,\vec{r}} d_{2,\vec{r}}). \end{aligned} \tag{D2}$$

Note that H_{HF} contains no anomalous terms. The conservation of the number of d particles, $\hat{N}_d = \sum_{\vec{r}} (d^{\dagger}_{1,\vec{r}} d_{1,\vec{r}} + d^{\dagger}_{2,\vec{r}} d_{2,\vec{r}})$, corresponds to the conservation of the total spin in the z direction in the original problem.

One can diagonalize (D2) by performing a unitary (Bogoliubov) transformation

$$\begin{pmatrix} \gamma_1 \\ \vdots \\ \gamma_N \\ \gamma_{N+1} \\ \vdots \\ \gamma_{2N} \end{pmatrix} = U \begin{pmatrix} d_{1,\vec{r}_1} \\ \vdots \\ d_{1,\vec{r}_N} \\ d_{2,\vec{r}_1} \\ \vdots \\ d_{2,\vec{r}_N} \end{pmatrix}. \tag{D3}$$

Here, U is a $2N \times 2N$ unitary matrix, and N is the number of lattice points. After this transformation, $H_{\mathrm{HF}} = \sum_{j=1}^{2N} E_j \gamma^{\dagger}_j \gamma_j$. Let us order the eigenstates such that $E_j < 0$ for $j = 1, \ldots, N_0$, where N_0 is the number of negative energies. Then, the many-body ground state can be written as a Slater determinant:

$$|\Psi\{\Delta_{\vec{r}}, \mu_{\vec{r}\sigma}\}\rangle = \prod_{j=1}^{N_0} \gamma^{\dagger}_j |\tilde{0}\rangle. \tag{D4}$$

Here, $|\tilde{0}\rangle = \prod_{\vec{r}} c^{\dagger}_{\vec{r}\downarrow} |0\rangle$ is defined as the vacuum state of the $d_{1,2}$ operators, and $|0\rangle$ is the original vacuum of the $c_{\uparrow,\downarrow}$ operators. Let us define W as an $N_0 \times N$ matrix containing the N_0 first rows of the matrix U. Then, one can verify that the overlap between two ground states is

$$\langle \Psi\{\Delta_{\vec{r}}, \mu_{\vec{r}\sigma}\} | \Psi\{\tilde{\Delta}_{\vec{r}}, \tilde{\mu}_{\vec{r}\sigma}\}\rangle = \det[W \tilde{W}^{\dagger}], \tag{D5}$$

where $\tilde{W}$ is the $N_0 \times N$ matrix corresponding to the occupied states in $|\Psi\{\tilde{\Delta}_{\vec{r}}, \tilde{\mu}_{\vec{r}\sigma}\}\rangle$.

APPENDIX E: STRONG-COUPLING EXPANSION

In the strong-coupling limit, $U/t \gg 1$, the physics of the negative-U Hubbard model is dominated by strongly bound pairs of electrons. We can use a Schrieffer-Wolff transformation to obtain an effective hard-core boson Hamiltonian for these pairs:

$$\begin{aligned} H_{\mathrm{eff}} = &\sum_{\langle i,j \rangle} \left[-J \left(S^x_i S^x_j + S^y_i S^y_j \right) + (J + J_a) S^z_i S^z_j \right] \\ &+ \sum_{\langle\langle i,j \rangle\rangle} \left[-J_2 \left(S^x_i S^x_j + S^y_i S^y_j \right) + J_2 S^z_i S^z_j \right] \\ &+ 12 J_{\mathrm{ring}} \sum_{i,jk} S^z_i S^z_j S^z_k - 2 J_{\mathrm{ring}} \sum_{i,jk} \left[S^z_i S^+_j S^-_k + \mathrm{H.c.} \right]. \end{aligned} \tag{E1}$$

The different couplings can be expressed as

$$J = \frac{2t^2}{U}, \quad J_2 = \frac{2t'^2}{U}, \quad J_a = 4V, \quad J_{\mathrm{ring}} = \frac{t' t^2}{U^2}. \tag{E2}$$

The first line in (E1) contains processes up to second order in t (t'). Note that this Hamiltonian is manifestly particle-hole symmetric at half filling *independently of* t'. The easiest way to see this is that the sublattice gauge transformation $e^{i \vec{Q} \cdot \vec{r}}$ with $Q = \{\pi, \pi\}$ appearing in the particle-hole transformation for the fermions is absent in the bosonic case as no fermionic signs have to be corrected for.

The first particle-hole symmetry breaking terms appear in third order in the hopping. In (E1) we only show those third-order terms that lead to such a symmetry breaking. They all contain J_{ring} where exactly one hopping takes place over a next-to-nearest neighbor bond. Note that we suppress the gauge field in (E1) for simplicity.

To study the effect of the particle-hole symmetry breaking terms $\propto t^2 t'$ we use exact diagonalization on clusters up to $L_x \times L_y = 4 \times 4$ using the hard-core boson model. We investigate the half-filled lattice and observe a degeneracy

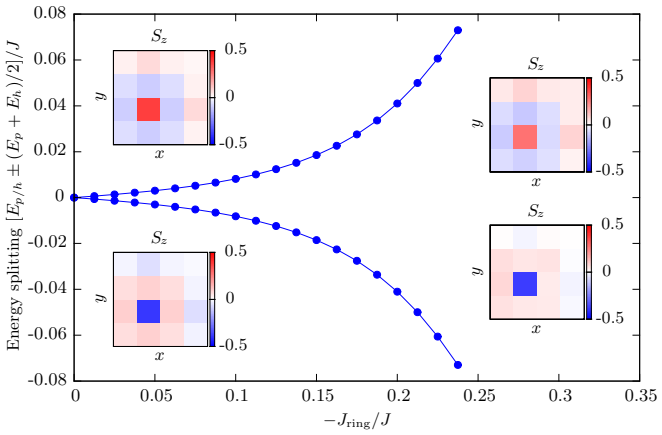

FIG. 7. (Color online) Strong coupling. Energy of the two lowest states at half filling in the hard-core boson model. At $t' = 0$ there is a degeneracy between two different vortices. At nonzero values of J_{ring} the particle-type condensate with a vortex with a density depletion forms in the ground state.

between two different vortex states at $t' = 0$ as expected; cf. Fig. 7. When turning on a $t'/t < 0$ as in the main text we find that the vortex with a density depletion is lower in energy. From this we conclude that the line where the integer p jumps from zero to -1 moves towards densities $n > 1$, in accordance with the results in the main text. These findings are also supported by the calculation of the Chern number [12]. For the actual calculations we used values for J_2, J_a, and J_{ring} that do not obey the rules (E2) for the following reason: Our aim is to study the breaking of particle-hole (PH) symmetry by the application of J_{ring} terms. For that we need a t' in the fermionic Hamiltonian. However, this induces also J_2, which does not break PH symmetry but which has to be counteracted by a larger J_a in order to fight the competing CDW. To keep the vortex smaller than the system size, we use $J = 1$, $J_2 = 0.2$, $J_a = 0.7$ and we change J_{ring} from 0 to 0.2. There is no reason to expect that by changing J_2 and J_a the main conclusion would change.

[1] N. Doiron-Leyraud, C. Proust, D. LeBoeuf, J. Levallois, J. B. Bonnemaison, R. Liang, D. A. Bonn, W. N. Hardy, and L. Taillefer, Nature (London) **447**, 565 (2007).

[2] D. LeBoeuf, N. Doiron-Leyraud, J. Levallois, R. Daou, J. B. Bonnemaison, N. E. Hussey, L. Balicas, B. J. Ramshaw, R. Liang, D. A. Bonn *et al.*, Nature (London) **450**, 533 (2007).

[3] D. LeBoeuf, N. Doiron-Leyraud, B. Vignolle, M. Sutherland, B. J. Ramshaw, J. Levallois, R. Daou, F. Laliberté, O. Cyr-Choinière, J. Chang *et al.*, Phys. Rev. B **83**, 054506 (2011).

[4] S. J. Hagen, C. J. Lobb, R. L. Greene, M. G. Forrester, and J. H. Kang, Phys. Rev. B **41**, 11630 (1990).

[5] A. van Otterlo, M. V. Feigel'man, V. B. Geshkenbein, and G. Blatter, Phys. Rev. Lett. **75**, 3736 (1995).

[6] K. Michaeli, K. S. Tikhonov, and A. M. Finkel'stein, Phys. Rev. B **86**, 014515 (2012).

[7] A. T. Dorsey, Phys. Rev. B **46**, 8376 (1992).

[8] J. Bardeen and M. J. Stephen, Phys. Rev. **140**, A1197 (1965).

[9] M. V. Feigel'man, V. B. Geshkenbein, A. I. Larkin, and V. M. Vinokur, Physica C **235**, 3127 (1994).

[10] N. H. Lindner, A. Auerbach, and D. P. Arovas, Phys. Rev. Lett. **102**, 070403 (2009).

[11] N. Lindner, A. Auerbach, and D. P. Arovas, Phys. Rev. B **82**, 134510 (2010).

[12] S. D. Huber and N. H. Lindner, Proc. Natl. Acad. Sci. USA **108**, 19925 (2011).

[13] J. E. Avron and R. Seiler, Phys. Rev. Lett. **54**, 259 (1985).

[14] T. Fukui, Y. Hatsugai, and H. Suzuki, J. Phys. Soc. Jpn. **74**, 1674 (2005).

[15] A. Paramekanti and A. Vishwanath, Phys. Rev. B **70**, 245118 (2004).

[16] M. Oshikawa, Phys. Rev. Lett. **84**, 1535 (2000).

[17] F. D. M. Haldane and Y.-S. Wu, Phys. Rev. Lett. **55**, 2887 (1985).

[18] In this statement, we have ignored the Goldstone modes in the superfluid phase, whose gap goes to zero as the system size increases. However, this gap is not expected to vary significantly as a function of Θ_x, Θ_y. Moreover, in a charged superconductor, there are no gapless Goldstone modes. One can imagine adding to the Hamiltonian (2) a repulsive long-range interaction which decays logarithmically with distance. This interaction gaps out the Goldstone modes. However, if the coefficient of the long-range interaction is sufficiently small, it does not affect the spectrum of the core much, and therefore it does not shift the position of the level crossing that occurs at the core.

[19] N. W. Ashcroft and N. D. Mermin, *Solid State Physics* (Harcourt, Orlando, 1987).

[20] J. E. Hoffman, E. W. Hudson, K. M. Lang, V. Madhavan, H. Eisaki, S. Uchida, and J. C. Davis, Science **295**, 466 (2002).